Molecules and Cells

Mislocalization of TORC1 to Lysosomes Caused by KIF11 Inhibition Leads to Aberrant TORC1 Activity

Yoon-Gu Jang[1,2,3], Yujin Choi[1,2,3], Kyoungho Jun[1,2], and Jongkyeong Chung[1,2,*]

[1]Institute of Molecular Biology and Genetics, Seoul National University, Seoul 08826, Korea, [2]School of Biological Sciences, Seoul National University, Seoul 08826, Korea, [3]These authors contributed equally to this work.
*Correspondence: jkc@snu.ac.kr
https://doi.org/10.14348/molcells.2020.0089
www.molcells.org

While the growth factors like insulin initiate a signaling cascade to induce conformational changes in the mechanistic target of rapamycin complex 1 (mTORC1), amino acids cause the complex to localize to the site of activation, the lysosome. The precise mechanism of how mTORC1 moves in and out of the lysosome is yet to be elucidated in detail. Here we report that microtubules and the motor protein KIF11 are required for the proper dissociation of mTORC1 from the lysosome upon amino acid scarcity. When microtubules are disrupted or KIF11 is knocked down, we observe that mTORC1 localizes to the lysosome even in the amino acid-starved situation where it should be dispersed in the cytosol, causing an elevated mTORC1 activity. Moreover, in the mechanistic perspective, we discover that mTORC1 interacts with KIF11 on the motor domain of KIF11, enabling the complex to move out of the lysosome along microtubules. Our results suggest not only a novel way of the regulation regarding amino acid availability for mTORC1, but also a new role of KIF11 and microtubules in mTOR signaling.

Keywords: *Drosophila*, KIF11, lysosome, microtubule, mTORC1

INTRODUCTION

A cell must decide whether it is the right time to run anabolic pathways for growth and proliferation according to its internal and external status. The mechanistic target of rapamycin complex 1 (mTORC1) lies at the center of the decision (Kim et al., 2013; 2019), and a myriad of signals including hormones and nutrients are converged to mTORC1, which promotes cell growth and division. When activated, mTORC1 directly phosphorylates ribosomal protein S6 kinase (S6K) and eukaryotic initiation factor 4E-binding protein 1 (4E-BP1) (Burnett et al., 1998; Chung et al., 1992). The phosphorylated and activated S6K phosphorylates ribosomal protein S6 (RpS6), whereas 4E-BP1 phosphorylation by mTORC1 frees the eukaryotic initiation factor 4E from its negative regulator, 4E-BP1.

Numerous signals that are responsible for regulating the activity of mTORC1 are relayed to a small G protein Ras homolog-enriched in the brain (RHEB) and its negative regulator TSC complex, which functions as a GTPase-activating protein of RHEB (Inoki et al., 2003). RHEB directly binds to mTORC1 to induce a global conformational change that increases its catalytic activity (Yang et al., 2017). Insulin growth factor signaling is probably one of the most-studied upstream cues, which upon activation frees RHEB from the TSC complex by Akt-dependent phosphorylation (Inoki et al., 2002; Menon et al., 2014).

Apart from the growth factor signaling, amino acids are required to fully activate mTORC1 (Hara et al., 1998; Wang et al., 1998). Unlike hormones that affect mTORC1 by inducing protein phosphorylation, the presence of amino acids triggers the movement of the complex from the cytosol to the lyso-

Received 7 April, 2020; revised 15 June, 2020; accepted 24 June, 2020; published online 7 August, 2020

eISSN: 0219-1032

some, the subcellular organelle where RHEB is constantly located. The main players that recruit mTORC1 to the lysosome are Rag GTPases (Nguyen et al., 2017; Sancak et al., 2010). RagA or B form a heterodimer with RagC or D, and the Rag complex is localized to the lysosome by the Ragulator complex. The Ragulator complex is a protein complex consisting of five subunits, which is attached to the cytosolic surface of the lysosome and binds to the C-terminal domains of RagA/B and RagC/D. When amino acids are present, RagA/B in the Rag complex is in GTP-bound form whereas RagC/D is GDP-bound. The Rag complex composed of GTP-bound RagA/B and GDP-bound RagC/D possesses a higher affinity with mTORC1 compared to the oppositely composed complex. Through extensive biochemical studies, some protein complexes lying upstream of the Rag complex are discovered including GTPase-activating proteins toward Rags complex (GATOR) 1 and 2 (Bar-Peled et al., 2013; Panchaud et al., 2013; Peng et al., 2017; Wolfson et al., 2017). Notably, not all amino acids are of equal importance, and the sensors for key signaling amino acids for activating mTORC1 have been revealed recently (Chantranupong et al., 2016; Saxton et al., 2016; Wolfson et al., 2016).

Microtubules and motor proteins are crucial for a variety of cellular events from maintaining cell structures and shape to cargo trafficking and cell division (Lee et al., 2019). Two members of the tubulin superfamily, α- and β-tubulins are the building blocks for microtubules, which are polymerized and depolymerized dynamically. Moving along microtubules are motor proteins, which walk through microtubules with their motor domains, for trafficking cargos or appropriately positioning microtubules during cell division. The motor proteins walking on microtubules fall into two kinds, kinesin motors which move from the minus-end to the plus-end (Porter et al., 1987; Vale et al., 1985) and dynein motors which move in the opposite direction (Paschal and Vallee, 1987) with several exceptional kinesins which move toward the minus-end (McDonald et al., 1990; Middleton and Carbon, 1994; Noda et al., 2001; Tseng et al., 2018; Walker et al., 1990).

Motor proteins are required for the movement of large protein complexes and intracellular components such as subcellular organelles. Both microtubules and actin filaments act as a track for the cargos to move along for long-distance and local transport, respectively (Gross, 2004). With each motor protein having its partner cargos, 45 kinesin-coding genes are classified into 14 families in mammals, and there are over 30 genes encoding dynein proteins reported to the current date (Hirokawa et al., 2009).

Motor proteins are also critical for cell division, as they participate in mitotic spindle aligning. One of the well-known mitotic motor proteins is KIF11, a member of the kinesin 5 families (Lawrence et al., 2004). KIF11 mainly regulates the assembly of the mitotic spindle (Cole et al., 1994; Enos and Morris, 1990; Slangy et al., 1995). KIF11 forms a bipolar homo-tetramer, which allows it to help two anti-parallel microtubules to be cross-linked, aligned, and able to glide appropriately with respect to each other (Kapitein et al., 2005; Kashlna et al., 1996; Sharp et al., 1999). Another study, however, suggested a different role of KIF11 in intracellular trafficking. In the study, KIF11 was proved to be involved in delivering CARTS (carriers of the trans-Golgi network [TGN] to the cell surface) from the TGN to the cell surface in non-mitotic cells (Wakana et al., 2013).

In a genetic screen for searching a previously unknown regulator of mTORC1, we have found that destabilizing microtubules increases TORC1 activity in *Drosophila*. Assuming that subcellular localization alteration can be a possible reason for the phenotype, we sought for the responsible motor protein and found that the suppression of *Klp61F*, a kinesin motor gene homologous to mammalian *KIF11*, also resulted in increased TORC1 activity. To study the molecular mechanism underlying this biology, we took advantage of the mammalian cell culture system. We confirmed that mislocalization of mTORC1 indeed occurred when microtubules were disrupted either genetically or pharmacologically or when *KIF11* was knocked down. We then identified that mLST8, a structural component of mTORC1, binds to the N-terminal motor domain of KIF11, linking the complex to the microtubules for the movement in the cell. In short, we here suggest a novel mechanism of the subcellular translocation of mTORC1 by microtubules and a specific motor protein KIF11, which allows regulation of mTORC1 activity regarding the amino acid availability.

MATERIALS AND METHODS

Drosophila husbandry and genetics

Species: *Drosophila melanogaster*. All flies were grown as indicated previously (Kim et al., 2017). w^{1118} strain was used as wild-type control. The following lines were obtained from the Bloomington *Drosophila* Stock Center (USA; in stock numbers): 44394, 51687, 35267, 35128, 41695, 33405, 38967, 32933, 33947, 34346, 28349, 28756, 54833, 67953, 38301, 31348, 36891, 31891, 54850, 53290, 35008, 55869, 67371, 33896, 65190, 63011, 44472, 58144, 36733, 35508, 29410, 50542, 35974, 43230, 67406, 35409, 40886, 43639, 28897, 5578, 40945, 35473, 36577, 35649, 28951, 35606, 32327, 35816, 42640, 35475, 33963, 35472, 64657, 64673, 36623, 62335, 51936, and *DE*-GAL4 (29650). The following lines were obtained from the Vienna *Drosophila* Resource Center (Austria; in stock numbers): 37087, 15992, 42008, 30679, 2955, 9396, 108863, 102379, 7716, 21863, 29182, 22412, 16078, 101755, 14705, 106667, 16986, 106812, 24934, 102525, 104536, 28369, 23715, 6261, 37991, 879, 29360, 2464, 30975, 101152, 13174, 102038, 41352, 108914, 22570, 330357, 52548, 109280, 27944, 40603, 44337, 108138, 45372, 110696, 110140, 46137, 23465, 52105, 35081, 48150, 41534, 36459, 110530, 48576, 18754, 27320, 101178, 28054, 108658, 101704, 32971, 105898, 41917, 19181, 27451, 32964, 27837, 35624, 48153, 102476, 19323, and UAS-*Arl2* RNAi (110627). $Arl2^{\Delta 309}$ was generously gifted by Dr. Hongyan Wang. The following stocks were obtained from the National Institute of Genetics (Japan; in stock numbers): 5520R-1, 18255R-1, 31014R-2, 9726R-1, and 31015R-1. Finally, the two stocks, 111083 and 111222, were obtained from the Kyoto Stock Center of *Drosophila* Genomics and Genetic Resources (Japan; in stock numbers).

For immunostaining *Drosophila* larval eye discs, wandering

larvae were used.

Clone generation

Clones of homozygous mutant cells were generated using *ey*-FLP-driven FRT recombination as described previously (Kim et al., 2017).

Generation of the allele *TBCC*^{45Ter}

A single guide RNA (sgRNA) was designed to target the early region of the coding sequence of *TBCC*. The forward sequence was: GAAAATCATGGAAGGCGACG (from 5' to 3'). The sgRNA sequence was cloned into pU6-Bbsl-chiRNA vector, which was injected to *w*^{1118} embryo together with pBS-Hsp70-Cas9 to induce double-strand break near the start codon. The mosaic adults hatched from the injected embryo (F_0) were crossed to balancer flies. Each F_1-derived from F_0 flies was again crossed to balancer flies and then tested whether it carries a mutant *TBCC* allele by sequencing, finally yielding a strain of a frame shift-induced early-stop allele, *TBCC*^{Ter45}.

Immunostaining

For immunostaining mammalian cells, cells were seeded on coverslips. Cells were fixed with 4% paraformaldehyde for 10 min at room temperature, and then permeabilized with 0.1% Triton X-100. After blocking in goat serum for 1 h, slides were incubated with primary antibody for 1 h at room temperature or at 4°C overnight, washed 3 times with phosphate-buffered saline (PBS), and then incubated with FITC- or TRITC-conjugated secondary antibodies (1:1,000; Invitrogen, USA) and Hoechst 33342 (blue) for 1 h at room temperature. The primary antibodies against LAMP2 (1:100, sc-18822; Santa Cruz Biotechnology, USA), mTOR (1:100, #2983; Cell Signaling Technology, USA), and β-tubulin (1:100, ab6046; Abcam, UK) were used for immunofluorescence. The slides were then washed 3 times with PBS and mounted. Cell images were captured with a confocal microscope (Zeiss, Germany).

For immunostaining *Drosophila* tissues, the anti-p-*Drosophila* RpS6 antibody generated in our lab was used as the primary antibody with the titer indicated previously (Kim et al., 2017). The same secondary antibodies were used as in mammalian cell immunostaining.

Mammalian cell culture, transfection and plasmids

HEK293E cells were cultured in DMEM (Welgene, Korea) supplemented with 10% fetal bovine serum (Invitrogen) at 37°C in a humidified atmosphere of 5% CO_2. For amino acid-starvation or stimulation, cells were seeded in 9.6 cm^2 6-well plates and incubated in media without or with amino acids, respectively. Cells were treated with 10 nM colchicine, 100 nM insulin, 200 nM rapamycin, 250 nM torin1 or U0126 for indicated hour(s). For immunostaining cells, cells were seeded in 3.5 cm^2 12-well plates and deprived of serum for 16 h before amino acid-starvation or stimulation. Cells were seeded in 9.6 cm^2 6-well plates and incubated in serum starved media for 16 h to identify serum-dependency. siRNAs for control (1003; Bioneer, Korea), *hTBCC* (6903-1; Bioneer), or *KIF11* (3832-1; Bioneer) were transfected to HEK293E cells using the RNAiMAX reagent (Invitrogen) according to the manufacture's protocol. For co-immunoprecipitation experiment, plasmids were transfected to HEK293E cells with polyethylenimine (408727; Sigma-Aldrich, USA) according to the manufacturer's protocol. The mammalian expression plasmids for human KIF11 were kind gifts from Dr. Wen H. Shen. KIF11 and mLST8 were cloned in pcDNA3.1 Flag, pcDNA3 Myc, or pEBG GST vectors. Plasmids for truncated forms of KIF11 were generated by polymerase chain reaction and cloned in pcDNA3.1 Flag expression vectors. All the constructs generated were confirmed by DNA sequencing.

Immunoblotting and immunoprecipitation assay

Cells were lysed in a lysis buffer (150 mM NaCl, 20 mM Tris, pH 7.4, 1 mM EGTA, 1 mM EDTA, 1% NP-40, 2.5 mM sodium pyrophosphate, 1 mM Na_3VO_4, 10% glycerol, protease inhibitors pepstatin A, PMSF, and leupeptin). Equivalent protein quantities were subjected to SDS-PAGE and transferred to nitrocellulose membranes. Membranes were blocked with 5% bovine serum albumin-containing PBS for 1 h at room temperature and then probed with the indicated primary antibodies, followed by the appropriate horseradish peroxidase (HRP)-conjugated anti-mouse/rabbit secondary antibodies. Immuno-reactive bands were visualized with enhanced chemiluminescence (ECL) reagent. For immunoprecipitation assay, cells were collected and lysed in 0.5 ml lysis buffer plus protease inhibitors for 30 min at 4°C. After 12,000*g* centrifugation for 15 min, the lysates were immunoprecipitated with 2 μg of specific antibody overnight at 4°C, and 30 μl A/G agarose beads were washed and then added for an additional 1 h. Thereafter, the precipitants were washed five times with the lysis buffer, and the immune complexes were boiled with loading buffer for 5 min and analyzed by SDS-PAGE. The following antibodies were used for immunoblotting and immunoprecipitation: antibodies against Flag (M185-3L; MBL Life Science, Japan), Myc (M192-3; MBL Life Science), GST (#2625; Cell Signaling Technology), p-S6K T389 (#9205; Cell Signaling Technology), S6K (#9202; Cell Signaling Technology), p-RpS6 (#2211; Cell Signaling Technology), RpS6 (#2217; Cell Signaling Technology), p-Akt Thr308 (#13038; Cell Signaling Technology), p-Akt Ser473 (#4060; Cell Signaling Technology), Akt (#9272; Cell Signaling Technology), and β-tubulin (E7; DSHB, USA).

Quantification and statistical analysis

All experiments were repeated at least three times, and all results were expressed as mean ± SD. Student's two-tailed *t*-test was used to determine statistical significance and Pearson's R-value was used to determine the degree of co-localization. For obtaining the value, 3 images per identical experimental condition containing 50 to 100 cells each were used. No regions of interest were specifically and manually designated: the entire image was used as it is. Software Prism 7 (GraphPad Software, USA) and Fiji were used for the statistical analyses.

RESULTS

Disrupted microtubule dynamics or suppression of the motor protein *Klp61F* results in increased TORC1 activity in *Drosophila*

As a previous work revealed a patterned activation of TORC1 in *Drosophila* eye disc (Kim et al., 2017), we performed a small-scale screen in search for an unknown regulator of TORC1 signaling in the tissue. For the screening pool, we consulted an open database, biophysical interactions of ORFeome-based complexes (BioPlex; http://bioplex.hms.harvard.edu/) to find possible interactors of Akt or the three TSC complex components, TSC1, TSC2, and TBC1D7. Our initial goal was to find a novel link between Akt and the TSC complex *in vivo*, and 26 human genes were chosen. A total of 68 UAS-RNAi lines targeting 34 *Drosophila* genes was prepared for the screen, and each of which was crossed to the flies carrying *DE*-GAL4 driver to allow RNAi expression in the dorsal region of *Drosophila* eye disc (Supplementary Table S1). The eye discs of third instar larvae were immunostained with anti-phospho-*Drosophila* RpS6 antibody for monitoring TORC1 activity. As we expressed RFP for labeling the cells with RNAi expression, we first examined and concluded that RFP expression alone does not have a phenotype regarding RpS6 phosphorylation (Supplementary Fig. S1).

Tubulin-binding cofactor C (*TBCC*) was the only gene that the knockdown by two independent UAS-RNAi lines resulted in increased RpS6 phosphorylation (Fig. 1A). *TBCC* is a ho-

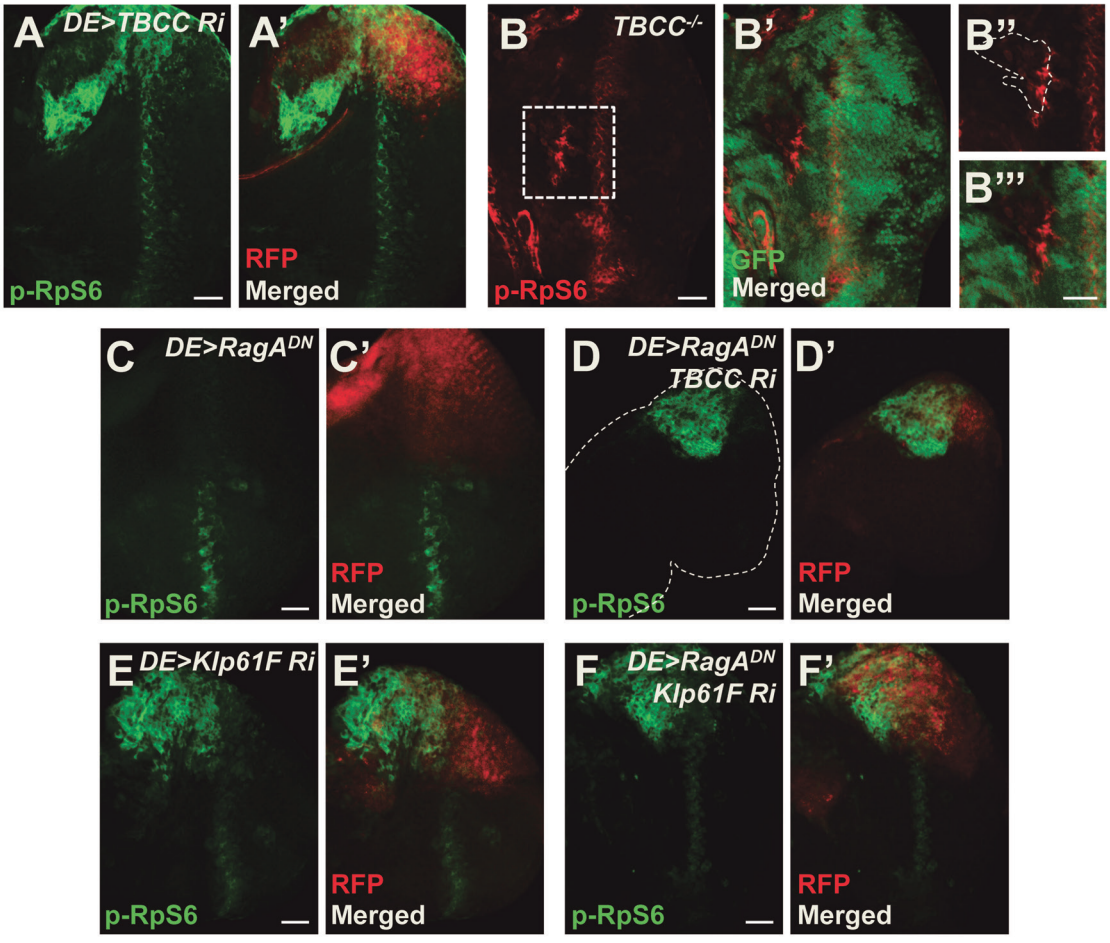

Fig. 1. Genetically disrupting microtubule dynamics or knocking down the motor protein *Klp61F* increases TORC1 activity in *Drosophila* eye disc. (A) *TBCC* was knocked down (*TBCC Ri*) in the dorsal region of *Drosophila* eye disc using dorsal-eye (*DE*)-GAL4 driver, labeled by RFP (red), and the tissue was immunostained with anti-p-*Drosophila* RpS6 antibody (green). Scale bar = 30 μm. (B) Clones of the cells with homozygous $TBCC^{45Ter}$ mutation indicated by the absence of GFP (green) were generated and the eye discs were immunostained with anti-p-*Drosophila* RpS6 antibody (red). Inset is magnified in the rightmost panels. Scale bars = 30 μm. (C and D) A dominant-negative form of RagA ($RagA^{DN}$) and/or RNAi-targeting *TBCC* (*TBCC Ri*) were expressed in the dorsal region of the eye disc as indicated in the panels, and the tissues were immunostained with anti-*Drosophila*-RpS6 antibody (green). The region of transgene expression was labeled by RFP (red). Scale bars = 30 μm. (E and F) $RagA^{DN}$ and/or RNAi-targeting *Klp61F* (*Klp61F Ri*) were expressed in the dorsal region of the eye disc as indicated in the panels and the tissues were immunostained with anti-*Drosophila* RpS6 antibody (green). The region of transgene expression was labeled by RFP (red). Scale bars = 30 μm.

molog for *RP2* in mammals, which is a disease-related gene. The loss of heterozygosity results in retinitis pigmentosa, a genetic eye disorder characterized by night vision difficulties and peripheral vision loss owing to the death of retinal cells (Li et al., 2013). Although a gene named *hTBCC*, which differs from *RP2*, exists in mammals as a paralog, *Drosophila TBCC* is the only homologous gene for both. To rule out the possibility that the result of the *TBCC* knockdown was due to an unknown off-targets, we generated a *TBCC* mutant *Drosophila* strain that carries an allele, $TBCC^{45Ter}$. This allele contains a frameshift starting from the 9th amino acid resulting in an early stop codon, only allowing a 45-amino acid protein instead of the wild-type protein with a length of 356 amino acids (Supplementary Fig. S2A). When homozygous mutant clones of $TBCC^{45Ter}$ were generated in the eye disc, TORC1 was found to be hyperactive in the clones, as it was in the cells with *TBCC* knockdown (Fig. 1B). Of note, in both TBCC knockdown and knockout eye discs, the TORC1 hyperactivity phenotype was clearly stronger in the anterior region cells than in the posterior region (Figs. 1A and 1B). As the protein TBCC is reported to function in microtubule synthesis (Nithianantham et al., 2015), we tested whether the effect

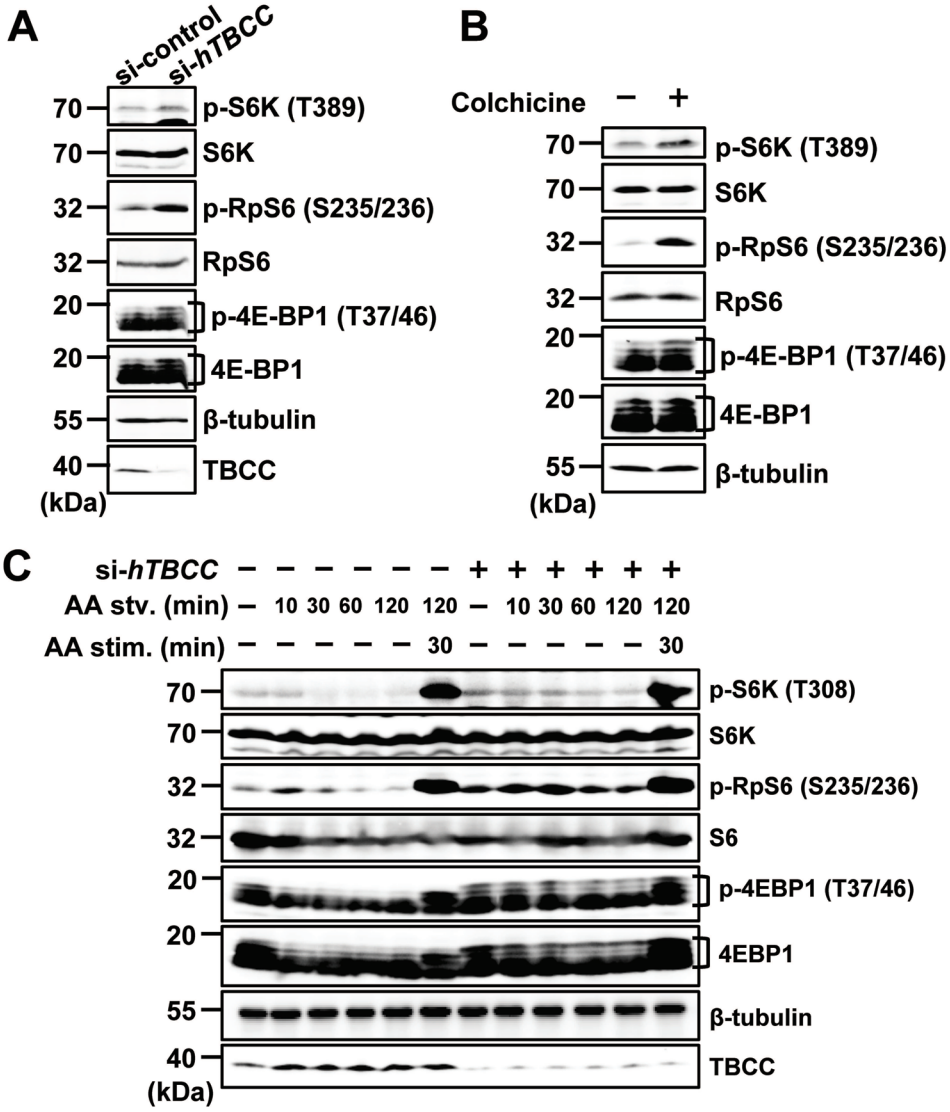

Fig. 2. Genetic or pharmacological suppression of microtubule dynamics increases mTORC1 activity in mammalian cells. (A) HEK293E cells were transfected with *hTBCC*-targeting siRNA (si-*hTBCC*) or a non-targeting control siRNA (si-control). The cell lysates were immunoblotted with anti-p-S6K, -S6K, -p-RpS6, -RpS6, -p-4E-BP1, -4E-BP1, -TBCC, and -β-tubulin antibodies. (B) HEK293E cells were treated with 10 μM colchicine (+) or distilled water (-) for 1 h and the cell lysates were immunoblotted with the same antibodies as in (A) except anti-TBCC antibody. (C) HEK293E cells were transfected with a non-targeting control siRNA (lanes 1-6) and *hTBCC*-targeting siRNA (lanes 7-12) and given amino acid-starvation (AA stv.) for indicated time. AA stim. indicates that the cells were provided with amino acids for 30 min after 2 h of amino acid-starvation. The cell lysate samples were immunoblotted with anti-p-S6K, -S6K, -p-RpS6, -RpS6, -p-4E-BP1, -4E-BP1, -TBCC, and -β-tubulin antibodies.

of *TBCC* knockdown we observed was due to microtubule dysfunction by depleting *Arl2*, which also participates in the synthesis of microtubules with the TBC family (Nithianantham et al., 2015). As in the knockdown of *TBCC*, *Arl2* knockdown or knockout also resulted in increased TORC1 activity (Supplementary Figs. S2B and S2C), suggesting that the phenotype was caused by the block of microtubule synthesis.

As microtubules are appreciated for the movement of intracellular cargos including protein complexes, we hypothesized that disrupting microtubules would increase mTORC1 activity by having it mislocalized in the cell. As the Rag complex is responsible for the lysosomal localization of mTORC1, we expressed a dominant-negative form of RagA ($RagA^{DN}$) with RNAi targeted for *TBCC* in the dorsal region of *Drosophila* eye disc. When $RagA^{DN}$ was expressed alone in the dorsal region, RpS6 phosphorylation decreased, ensuring signals from amino acids are a prerequisite for RpS6 phosphorylation in the eye disc (Fig. 1C). When $RagA^{DN}$ and *TBCC* RNAi were simultaneously expressed in the dorsal region, RpS6 phosphorylation was higher, similar to expressing *TBCC* RNAi alone. This suggests that *TBCC* knockdown can increase TORC1 activity even when the Rag complex has a low affinity toward TORC1 (Figs. 1C and 1D).

We moved on to another question of whether there is a motor protein responsible for the movement of mTORC1 along microtubules in the cell. Given the data indicating the lysosome-to-cytosol movement of mTORC1 through microtubules, we hypothesized that knockdown of the motor protein would increase RpS6 phosphorylation and render resistance of mTORC1 activity during amino acid starvation. We also predicted that the motor protein would have a direct physical interaction with mTORC1. To find out the motor protein involved, we have done a genetic screen using *DE*-GAL4 and UAS-RNAi targeting for each of *Drosophila* motor protein genes, in search for any candidate that elicits ectopic RpS6 phosphorylation. Among 27 kinesin-coding genes and 13 dynein-coding ones, *Klp61F* knockdown was observed to increase RpS6 phosphorylation (Fig. 1E, Supplementary Table S2). Moreover, like *TBCC* knockdown, *Klp61F* knockdown with concomitant expression of $RagA^{DN}$ showed elevated RpS6 phosphorylation (Fig. 1F).

mTORC1 activity is resistant to amino acid starvation when microtubules are disrupted in mammalian cells

We then tested whether the phenotype could be observed in mammalian cells. When HEK293E cells were treated with siRNA-targeting *hTBCC*, the phosphorylation of RpS6, S6K, and 4E-BP1 was increased (Fig. 2A) in consistent with the results from *Drosophila* tissues. The pharmacologically inhibition of the of microtubule synthesis is another way in which we could test whether destabilizing microtubules indeed causes hyperactive mTORC1. In Drosophila eye discs, it was, however, difficult to apply this approach, including *ex vivo* drug treatment, because, after dissection, RpS6 dephosphorylation occurred too rapidly. Hence, any delay due to the drug treatment before fixation ended up with totally disappeared RpS6 phosphorylation regardless of experimental conditions. In mammalian cells, however, treating chemicals was much feasible, which allowed us to use colchicine, a microtubule destabilizer. After confirming that employing colchicine did induce microtubule destabilization (Supplementary Fig. S3), we tested whether inhibiting microtubule polymerization was the actual cause of the phenotype. Indeed, when colchicine was added to cells, mTORC1 activity increased significantly (Fig. 2B).

Subsequently, mTORC1 activity was measured in mammalian cells starved by administering an amino acid-free medium with or without *hTBCC* knockdown. As a result, the cells with *hTBCC* knockdown were significantly resistant to amino acid retrieval in terms of mTORC1 activity (Fig. 2C). We could consistently detect higher levels of phosphorylated S6 and 4E-BP1 in the siRNA-treated group (Fig. 2C). Notably, amino acid stimulation following starvation allowed a similar peak of mTORC1 activity in both control and microtubule-disrupted cells, indicating that even after microtubule disruption, activation of mTORC1 by amino acids is still available.

mTORC1 localizes to the lysosome under amino acid starvation when microtubules are disrupted

We then immunostained mTOR and LAMP2, markers of mTORC1 and lysosomes, respectively, in various conditions in order to confirm that microtubules regulate the subcellular localization of mTORC1 according to amino acid availability. In the control group, as expected, the two marker proteins only co-localized when cells were stimulated by amino acids (Figs. 3A and 3B, 3F and 3G). In experimental groups, however, both *hTBCC* knockdown and pharmacological inhibition of microtubule polymerization also led to a stronger colocalization of the two proteins even when the cells were placed in an amino acid-free medium (Figs. 3C and 3D, 3H and 3I, respectively). The Pearson's R-value indicating the degree of co-localization between mTOR and LAMP2 was plotted to quantify the results (Figs. 3E and 3J). In consistence with the result that amino acid stimulation further increased mTORC1 activity when *hTBCC* was knocked down (Fig. 2C), the co-localization coefficient was peaked to a similar level in both control and experimental groups (Figs. 3E and 3J). This again suggested that although blocking microtubule polymerization led to a higher mTORC1 activity, it still had a capability of being more activated by further stimulation such as amino acid replenishment.

mTORC1 becomes resistant to amino acid starvation when *KIF11* is knocked down in mammalian cells

As *KIF11* is the mammalian homolog of *Klp61F*, we knocked down *KIF11* in HEK293E cells and tested whether the phosphorylation of RpS6 or S6K is altered. As expected, when cells had *KIF11* knocked down, RpS6, S6K, and 4E-BP1 phosphorylation increased compared to those of control cells (Fig. 4A). We then questioned whether *KIF11* knockdown renders resistance of mTORC1 to amino acid starvation in the same fashion to microtubule destabilization. Hence, we placed the cells under time-series amino acid-starvation with or without *KIF11* knockdown (Fig. 4B). When amino acid-starvation was given, the phosphorylation of RpS6 decreased to a lesser extent compared to that of control cells. Although the difference was not as great, the phosphorylation of S6K was also observed to be more resistant. Moreover, the phosphoryla-

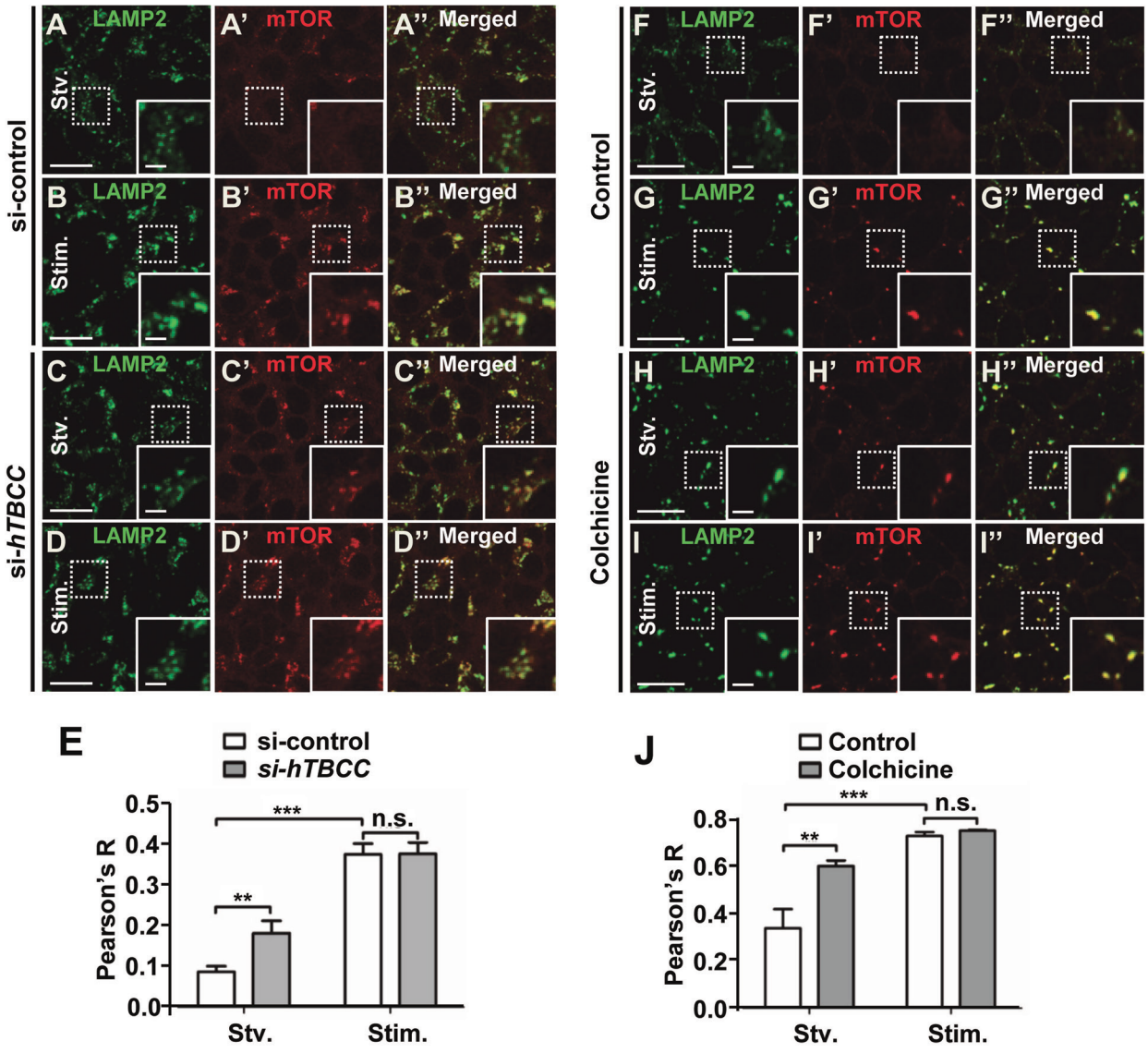

Fig. 3. mTORC1 is forced to the lysosome upon amino acid-starvation when microtubules are destabilized. (A-D) HEK293E cells were transfected with a non-targeting control siRNA (si-control; A and B) and *hTBCC*-targeting siRNA (si-*hTBCC*; C and D), and given amino acid-starvation for 1 h (Stv.; A and C) or provided with amino acids for 30 min after being starved for 1 h (Stim.; B and D). The cells were immunostained with anti-LAMP2 (green) and -mTOR (red) antibodies. The area boxed by dotted lines is enlarged in the inset at bottom right of each panel. Scale bars = 20 μm or 5 μm (inset). (E) The degree of co-localization between mTOR and LAMP2 were quantified in 500 cells from three independent experiments in each group. All results were expressed as mean ± SD. Probabilities: $^{**}P < 0.01$ and $^{***}P < 0.001$, calculated by Student's two-tailed *t*-test. n.s., not significant. (F-I) HEK293E cells were under amino acid-starvation for 1 h (Stv.; F and H) or provided with amino acids for 30 min after being starved for 1 h (Stim.; G and I). Distilled water (Control; F and G) or 10 μM colchicine (Colchicine; H and I) was treated for 1 h (Stv.) or 1.5 h (Stim.) and the cells were immunostained with anti-LAMP2 (green) and -mTOR (red) antibodies. The area boxed by dotted lines is enlarged in the inset at bottom right of each panel. Scale bars = 20 μm or 5 μm (inset). (J) The degree of co-localization between mTOR and LAMP2 were quantified in 300 cells from three independent experiments in each group. All results were expressed as mean ± SD. Probabilities: $^{**}P < 0.01$ and $^{***}P < 0.001$, calculated by Student's two-tailed *t*-test.

tion of both proteins was even higher when cells were stimulated with amino acids, indicating that the *KIF11* knockdown did not induce mTORC1 activity to the maximum. Also, phosphorylation of 4E-BP1 was higher in cells with a decreased level of *KIF11*. These data were consistent with the results from microtubule destabilization experiments, suggesting the relevance between microtubules and KIF11 in regulating mTORC1 signaling activity (see Fig. 2). At this point, to further verify essential amino acids and subcellular localization of mTORC1, we ruled out any possibility regarding the involvement of microtubule destabilization or KIF11 inhibition in the increased mTORC1 activity through insulin growth

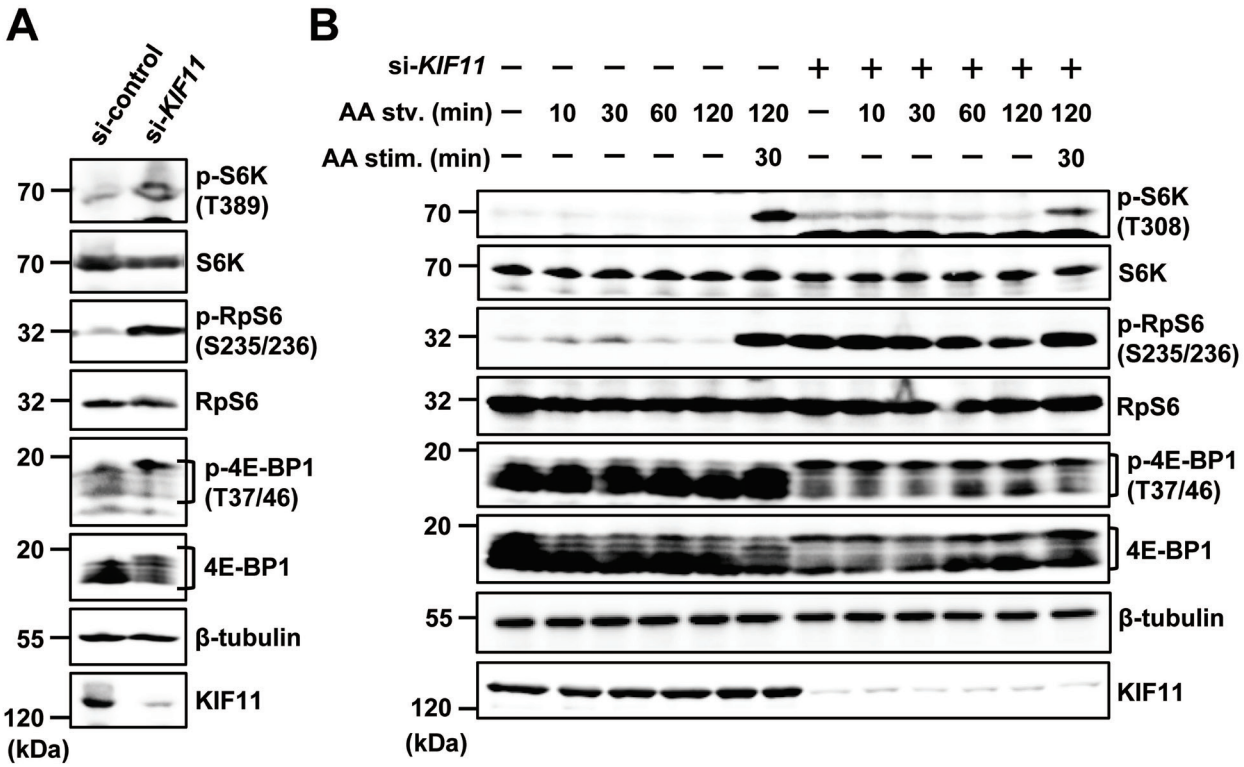

Fig. 4. Knockdown of *KIF11* results in sustained mTORC1 activity after amino acid-starvation in a similar fashion to microtubule destabilization. (A) HEK293E cells were transfected with *KIF11*-targeting siRNA (si-*KIF11*) or a non-targeting control siRNA (si-control) and the cell lysate samples were immunoblotted with anti-p-S6K, -S6K, -p-RpS6, -RpS6, -p-4E-BP1, -4E-BP1, -KIF11, and -β-tubulin antibodies. (B) HEK293E cells were transfected with a non-targeting control siRNA (lanes 1-6) and *KIF11*-targeting siRNA (lanes 7-12) and given amino acid-starvation (AA stv.) for indicated time. AA stim. indicates that the cells were provided with amino acids for 30 min after 2 h of amino acid-starvation. The cell lysate samples were immunoblotted with anti-p-S6K, -S6K, -p-RpS6, -RpS6, -p-4E-BP1, -4E-BP1, -KIF11, and -β-tubulin antibodies.

factor signaling pathway. Expectedly, disrupting microtubules or knocking down *KIF11* did not lead to sustained S6K or RpS6 phosphorylation in cells under serum-free media. This suggests that the regulation of mTORC1 by the PI3K-TSC complex-RHEB axis is independent of microtubules and KIF11 motor protein (Supplementary Fig. S4).

As we have done in the case of microtubule destabilization, the subcellular localization of mTORC1 was monitored by labeling mTOR and LAMP2 in *KIF11* siRNA-treated cells. Compared to control cells, far more cells showed co-localized mTOR and LAMP2 even in an amino acid-free condition with *KIF11* knocked down (Figs. 5A-5D). The Pearson's R-value indicated that the cells with *KIF11* knockdown showed a high co-localization as the controls with amino acid stimulation (Fig. 5E). Taken together, although destabilizing microtubules or inhibiting the motor protein KIF11 showed somewhat different degrees of phenotypes, the results were all consistent, suggesting that microtubules and KIF11 are required for the alteration of mTORC1 subcellular localization induced by amino acid scarcity in mammalian cells.

Through its motor domain, KIF11 binds to and regulates mTORC1

To further speculate how KIF11 interacts with mTORC1, we performed co-immunoprecipitation assays. In an open database BioGRID (https://thebiogrid.org/), KIF11 was reported to bind mLST8, a member of mTORC1, which led us to test the interaction between KIF11 and mLST8. Indeed, Myc-tagged mLST8 was co-immunoprecipitated with Flag-tagged KIF11 (Fig. 6A). Moreover, when we tested whether KIF11 interacts with other components of mTORC1, we found that, like mLST8, RAPTOR and mTOR were co-immunoprecipitated with KIF11 (Supplementary Fig. S5). We then sought for the region of the interaction using truncated forms of KIF11 and full-length mLST8. Interestingly, the N-terminal motor domain of KIF11 was found to be important for the interaction between KIF11 and mLST8 (Fig. 6B). These results suggest that KIF11 binds to mTORC1 through its N-terminal motor domain.

To investigate which one of the two mTOR-containing complexes is responsible for the increased phosphorylation of RpS6 and S6K upon *KIF11* or *hTBCC* knocked down, we first treated rapamycin, an acute mTORC1-specific inhibitor (Heitman et al., 1991), to the cell. Treating rapamycin dramatically reduced phosphorylation of RpS6 but increased S6K by KIF11 and hTBCC knockdown (Fig. 6C). Interestingly, in conditions where *KIF11* or *hTBCC* was knocked down, rapamycin treatment could not reduce RpS6 phosphorylation completely as

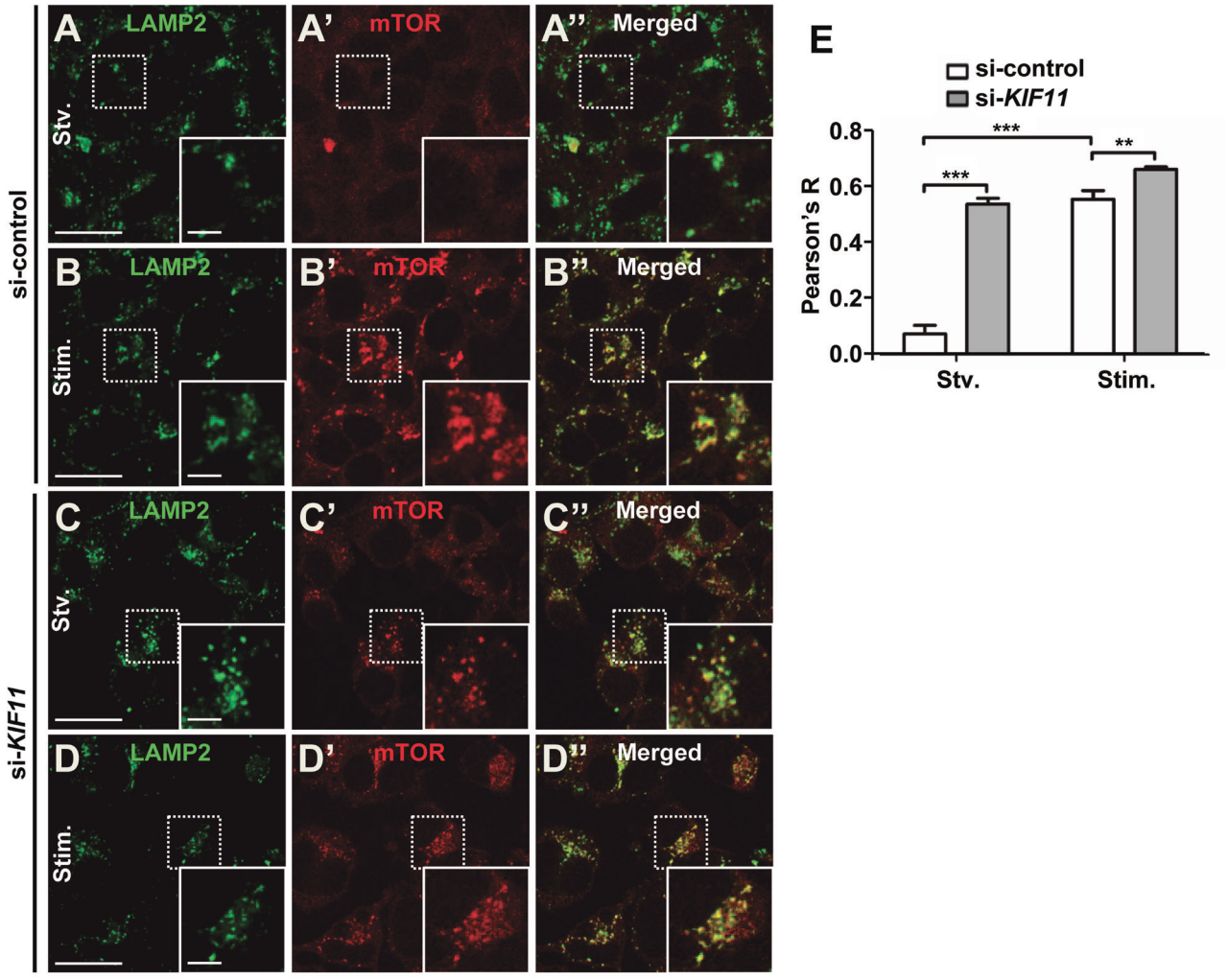

Fig. 5. mTORC1 is forced to localize to lysosomes under amino acid starvation when *KIF11* is depleted. (A-D) HEK293E cells were transfected with a non-targeting control siRNA (si-control; A and B) or *KIF11*-targeting siRNA (si-*KIF11*; C and D), and given amino acid-starvation for 1 h (Stv.; A and C) or provided with amino acids for 30 min after being starved for 1 h (Stim.; B and D). The cells were immunostained with anti-LAMP2 (green) and -mTOR (red) antibodies. The area boxed by dotted lines is enlarged in the inset at bottom right of each panel. Scale bars = 20 μm or 5 μm (inset). (E) The degree of co-localization between mTOR and LAMP2 were quantified in 300 cells from three independent experiments in each group. All results were expressed as mean ± SD. Probabilities: $^{**}P < 0.01$ and $^{***}P < 0.001$, calculated by Student's two-tailed *t*-test.

in the control condition. Also, the increased phosphorylation of RpS6 and S6K due to *KIF11* or *hTBCC* depletion was successfully decreased by torin1, a drug that inhibits both mTORC1 and mTORC2 (Fig. 6D). Note that in the groups without rapamycin or torin1 treatment, cells possessed a high level of phosphorylation for S6K and RpS6 regardless of *hTBCC* or *KIF11* knockdown. This is because the cell medium was changed upon the drug treatment, boosting mTORC1 activity (Figs. 6C and 6D). To identify whether the activity of mTORC2 was changed upon microtubule destabilization or *KIF11* knockdown, we examined the phosphorylation of Akt Ser473, a residue known to be phosphorylated by mTORC2 (Sarbassov et al., 2005). Whereas microtubule disruption and *KIF11* depletion consistently induced RpS6 phosphorylation, Akt Ser473 phosphorylation was unaffected in all conditions (Fig. 6E). With these results, we concluded that microtubule and KIF11 regulate the phosphorylation of RpS6 and S6K depending on mTORC1 mainly, but not by mTORC2. Besides, to find out whether RSK was also responsible for increased phosphorylation of RpS6 upon microtubule disruption, we treated U0126, a MEK-specific inhibitor, along with *KIF11* knockdown to suppress RSK at the upstream. Interestingly, the RpS6 phosphorylation was still high in the cells treated with both U0126 and *KIF11*-targeting siRNA (Supplementary Fig. S6), indicating that the activity of RSK and MAP kinase was dispensable in the phenomenon which we observed with *KIF11* depletion.

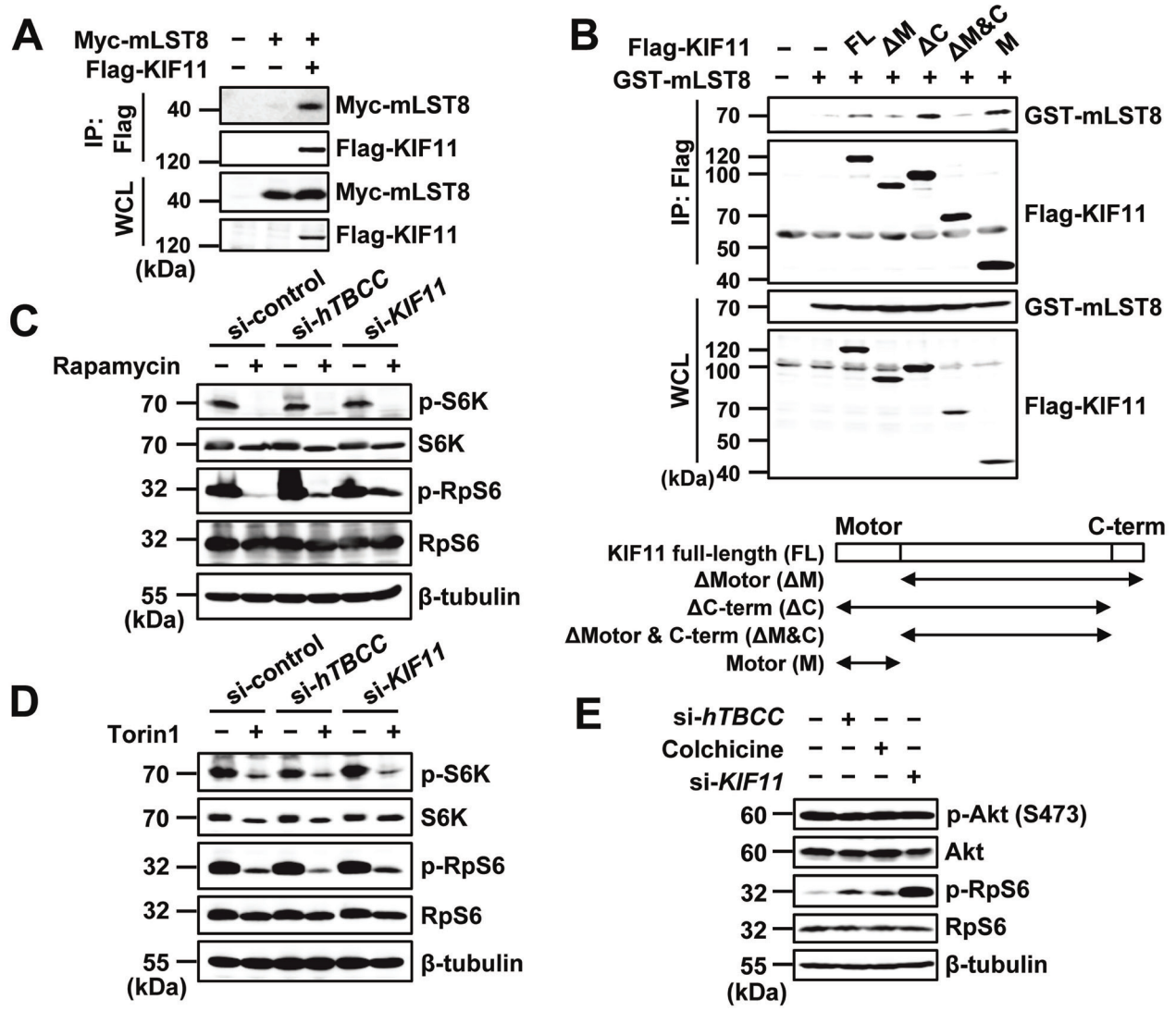

Fig. 6. KIF11 binds to mTORC1 through its motor domain. (A) Flag-tagged KIF11 and Myc-tagged mLST8 were co-expressed in HEK293E cells. The lysate samples were immunoprecipitated with anti-Flag antibody and immunoblotted with anti-Myc and -Flag antibodies. Whole cell lysate (WCL) samples were loaded to confirm protein expression levels. Flag-tagged vector and Myc-tagged vector were transfected as negative controls (-). (B) Full-length or truncated form of Flag-tagged KIF11 was co-expressed with GST-tagged mLST8 in HEK293E cells. The lysate samples were immunoprecipitated with anti-Flag antibody and immunoblotted with anti-GST and -Flag antibodies. WCL samples were loaded to confirm protein expression levels. Flag-tagged vector and GST-tagged vector were transfected as negative controls (-). The cartoon in the lower part of the panel depicts how each truncated form of KIF11 was generated. (C) HEK293E cells with *hTBCC* or *KIF11* knockdown (si-*hTBCC* and si-*KIF11*, respectively) were treated with new medium which contains DMSO (-) or 200 nM rapamycin (+) for 1 h. The cell lysate samples were immunoblotted with anti-p-S6K, -S6K, -p-RpS6, -RpS6, and -β-tubulin antibodies. (D) HEK293E cells with *hTBCC* or *KIF11* knockdown (si-*hTBCC* and si-*KIF11*, respectively) were treated with new medium which contains DMSO (-) or 250 nM torin1 (+) for 1 h. The cell lysate samples were immunoblotted with the same antibodies as in (C). (E) HEK293E cells were transfected with *hTBCC* or *KIF11* knockdown (si-*hTBCC* and si-*KIF11*, respectively) or treated with 10 μM colchicine for 1 h. The cell lysate samples were immunoblotted with anti-p-RpS6, -RpS6, -p-Akt (Ser473), -Akt, and -β-tubulin antibodies.

DISCUSSION

This study highlights the role of microtubules and a specific motor protein KIF11 on the subcellular movement of mTORC1 from the lysosome to the cytosol. The inhibition of microtubule polymerization, either done genetically or pharmacologically, results in aberrant mTORC1 activity *in vivo* and *in vitro*, suggesting the possibility of mTORC1 being transported along microtubules. Moreover, we have verified a motor protein KIF11, which binds to mTORC1, as the actual transporter of the complex. Notably, KIF11 has extensively been appreciated as a mitotic kinesin having a role in mitotic spindle assembly. We, therefore, suggest that, along with its role in mitosis, KIF11is also engaged in protein complex

transporting. Interestingly, this is not the first report of KIF11 concerning cargo trafficking, as a previous study already suggested a role in the post-Golgi secretory pathway (Wakana et al., 2013).

In the dorsal region of Drosophila eye disc, ectopic expression of RNAi targeting TBCC or Klp61F was applied for disrupting microtubules or depleting Klp61F, respectively. Interestingly, the higher TORC1 activity caused by such genetic manipulations was mainly restricted to cells in the anterior region (see Figs. 1A and 1B, 1D-1F). This different responsiveness is possible because of the different repertoire of regulation on TORC1 in the eye disc regarding the location. This is not the only case in which cells with different differentiation status responded differently to genetic manipulations intended to alter TORC1 activity. For example, when a constitutively active form of insulin receptor or myristoylated Akt was expressed clonally in the eye disc, only cells near the second mitotic wave (the cells positive for phosphorylated RpS6 in the wild-type eye disc) showed higher RpS6 phosphorylation (Supplementary Fig. S7).

As the microtubule/KIF11-dependent movement of mTORC1 enhances its activity in both normal and amino acid-starved conditions, we assume this movement occurs specifically when mTORC1 is moving out of the lysosome. This is further ensured by the fact that stimulating the starved cells by amino acids increases mTORC1 activity regardless of microtubule stability or KIF11 availability. This means that the complex coming to the lysosome was not affected by those factors. In short, the movement of mTORC1 through microtubules via KIF11 is in a one-way fashion, allowing the complex to move out of the lysosome. The microtubule- and motor protein-independent way of mTORC1 translocating from the cytosol to the lysosome would be an interesting topic to pursue in the future. In contrast to our expectation that mTORC1 would bind to the C-terminus of KIF11 like a typical cargo trafficking using a kinesin motor dimer, mLST8 was found to bind KIF11 through the motor domain (Fig. 6B). As KIF11 is known to work in a homo-tetrameric manner for the mitosis (Mann and Wadsworth, 2019), we suspect that when trafficking mTORC1, one end of tetramer would bind to the microtubule and the other to mLST8. Especially, electron microscopy explaining the binding of the two would provide valuable information. Indeed, a research indicated that the bipolar assembly (BASS) domain of KLP61F is critical in the formation of homo-tetramer (Scholey et al., 2014). This research also noticed that multiple KLP61F mutants in the BASS domain form monomer or dimer, but not tetramer. Therefore, a further research is needed to verify whether mTORC1 translocation is affected by KIF11/KLP61F mutants which are unable to form tetramers.

The physiological meaning of the movement of mTORC1 by the motor protein KIF11 is yet elucidated. Since mTROC1 activity control involves a change in mTORC1 localization between the lysosome and the cytosol according to amino acid availability, the simplest answer for why mTORC1 is transported between these spaces through microtubules would be by detaching the complex from its activation base camp. There are, however, other possibilities as well. According to recent studies, the subcellular localization of mTORC1 does not perfectly correspond to its regulation by amino acids (Manifava et al., 2016). In the article, the authors showed that when amino acid stimulation induces lysosomal localization of mTORC1, the complex gets out of the lysosome quickly, and mTORC1 activity did not fall immediately after the detachment. This suggests the localization of the complex has more to do than just activity regulation. We, therefore, cannot rule out the possibility that mTORC1 is transported to a place other than lysosomes for a purpose that is not activity regulation.

Collectively, this study consistently indicates that microtubules and KIF11 are required for a proper movement of mTORC1 from the lysosome to the cytosol in response to amino acid starvation and mTROC1 hyperactivation upon the blockage of the transport system. As there is some room for further investigation of this phenomenon, further studies will provide valuable information on how this critical signaling pathway is delicately regulated by changes in subcellular localization of mTORC1.

Note: Supplementary information is available on the Molecules and Cells website (www.molcells.org).

ACKNOWLEDGMENTS

We would like to thank Dr. Hongyan Wang for kindly providing the *Arl2*$^{\Delta 309}$ *Drosophila* stock and the four stock centers, Bloomington *Drosophila* Stock Center, Vienna *Drosophila* Resource Center, National Institute of Genetics, and *Drosophila* Genomics and Genetic Resources. We are grateful to Dr. Wen H. Shen for providing us with KIF11 constructs. We also would like to appreciate all the members of the Chung lab for helpful and critical discussions. This research was supported by a grant from the National Research Foundation of Korea (NRF-2019R1A2C2005810). Y.G.J. and Y.C. were supported by the BK21 Plus Program from the Ministry of Education, Republic of Korea.

AUTHOR CONTRIBUTIONS

J.C. funding acquisition; J.C. and Y.G.J. conceptualization; J.C. supervision; Y.G.J. and Y.C. investigation; Y.G.J. and Y.C. visualization; Y.G.J. and Y.C. writing - original draft; J.C., Y.G.J., Y.C., and K.J. writing - review & editing.

CONFLICT OF INTEREST

The authors have no potential conflicts of interest to disclose.

ORCID

Yoon-Gu Jang http://orcid.org/0000-0002-4773-6053
Yujin Choi http://orcid.org/0000-0002-0699-6211
Kyoungho Jun http://orcid.org/0000-0001-5317-5531
Jongkyeong Chung http://orcid.org/0000-0001-5894-7537

REFERENCES

Bar-Peled, L., Chantranupong, L., Cherniack, A.D., Chen, W.W., Ottina, K.A., Grabiner, B.C., Spear, E.D., Carter, S.L., Meyerson, M., and Sabatini, D.M. (2013). A Tumor suppressor complex with GAP activity for the Rag GTPases that signal amino acid sufficiency to mTORC1. Science *340*, 1100-1106.

Burnett, P.E., Barrow, R.K., Cohen, N.A., Snyder, S.H., and Sabatini, D.M. (1998). RAFT1 phosphorylation of the translational regulators p70 S6

kinase and 4E-BP1. Proc. Natl. Acad. Sci. U. S. A. *95*, 1432-1437.

Chantranupong, L., Scaria, S.M., Saxton, R.A., Gygi, M.P., Shen, K., Wyant, G.A., Wang, T., Harper, J.W., Gygi, S.P., and Sabatini, D.M. (2016). The CASTOR proteins are arginine sensors for the mTORC1 pathway. Cell *165*, 153-164.

Chung, J., Kuo, C.J., Crabtree, G.R., and Blenis, J. (1992). Rapamycin-FKBP specifically blocks growth-dependent activation of and signaling by the 70 kd S6 protein kinases. Cell *69*, 1227-1236.

Cole, D.G., Saxton, W.M., Sheehan, K.B., and Scholey, J.M. (1994). A "slow" homotetrameric kinesin-related motor protein purified from Drosophila embryos. J. Biol. Chem. *269*, 22913-22916.

Enos, A.P. and Morris, N.R. (1990). Mutation of a gene that encodes a kinesin-like protein blocks nuclear division in A. nidulans. Cell *60*, 1019-1027.

Gross, S.P. (2004). Hither and yon: a review of bi-directional microtubule-based transport. Phys. Biol. *1*, R1-R11.

Hara, K., Yonezawa, K., Weng, Q.P., Kozlowski, M.T., Belham, C., and Avruch, J. (1998). Amino acid sufficiency and mTOR regulate p70 S6 kinase and eIF-4E BP1 through a common effector mechanism. J. Biol. Chem. *273*, 14484-14494.

Heitman, J., Movva, N.R., and Hall, M.N. (1991). Targets for cell cycle arrest by the immunosuppressant rapamycin in yeast. Science *253*, 905-909.

Hirokawa, N., Noda, Y., Tanaka, Y., and Niwa, S. (2009). Kinesin superfamily motor proteins and intracellular transport. Nat. Rev. Mol. Cell Biol. *10*, 682-696.

Inoki, K., Li, Y., Xu, T., and Guan, K.L. (2003). Rheb GTPase is a direct target of TSC2 GAP activity and regulates mTOR signaling. Genes Dev. *17*, 1829-1834.

Inoki, K., Li, Y., Zhu, T., Wu, J., and Guan, K.L. (2002). TSC2 is phosphorylated and inhibited by Akt and suppresses mTOR signalling. Nat. Cell Biol. *4*, 648-657.

Kapitein, L.C., Peterman, E.J., Kwok, B.H., Kim, J.H., Kapoor, T.M., and Schmidt, C.F. (2005). The bipolar mitotic kinesin Eg5 moves on both microtubules that it crosslinks. Nature *435*, 114.

Kashlna, A., Baskin, R., Cole, D., Wedaman, K., Saxton, W., and Scholey, J. (1996). A bipolar kinesin. Nature *379*, 270.

Kim, M.Y., Kruger., A.J., Jeong, J.Y., Kim, J., Shin, P.K., Kim, S.Y., Cho, J.Y., Hahm, K.B., and Hong, S.P. (2019). Combination therapy with a PI3K/mTOR dual inhibitor and chloroquine enhances synergistic apoptotic cell death in Epstein–Barr virus-infected gastric cancer cells. Mol. Cells *42*, 448-459.

Kim, S.G., Buel, G.R., and Blenis, J. (2013). Nutrient regulation of the mTOR complex 1 signaling pathway. Mol. Cells *35*, 463-473.

Kim, W., Jang, Y.G., Yang, J., and Chung, J. (2017). Spatial activation of TORC1 is regulated by Hedgehog and E2F1 signaling in the Drosophila eye. Dev. Cell *42*, 363-375.e4.

Lawrence, C.J., Dawe, R.K., Christie, K.R., Cleveland, D.W., Dawson, S.C., Endow, S.A., Goldstein, L.S., Goodson, H.V., Hirokawa, N., Howard, J., et al. (2004). A standardized kinesin nomenclature. J. Cell Biol. *167*, 19-22.

Lee, J., Yi, S., Chang, J.Y., Kim, J.T., Sul, H.J., Park, K.C., Zhu, X., Cheng, S.Y., Kero, J., Kim, J., et al. (2019). Loss of primary cilia results in the development of cancer in the murine thyroid gland. Mol. Cells *42*, 113-122.

Li, L., Khan, N., Hurd, T., Ghosh, A.K., Cheng, C., Molday, R., Heckenlively, J.R., Swaroop, A., and Khanna, H. (2013). Ablation of the X-linked retinitis pigmentosa 2 (Rp2) gene in mice results in opsin mislocalization and photoreceptor degeneration. Invest. Ophthalmol. Vis. Sci. *54*, 4503-4511.

Manifava, M., Smith, M., Rotondo, S., Walker, S., Niewczas, I., Zoncu, R., Clark, J., and Ktistakis, N.T. (2016). Dynamics of mTORC1 activation in response to amino acids. Elife *5*, e19960.

Mann, B.J. and Wadsworth, P. (2019). Kinesin-5 regulation and function in mitosis. Trends Cell Biol. *29*, 66-79.

McDonald, H.B., Stewart, R.J., and Goldstein, L.S. (1990). The kinesin-like ncd protein of Drosophila is a minus end-directed microtubule motor. Cell *63*, 1159-1165.

Menon, S., Dibble, C.C., Talbott, G., Hoxhaj, G., Valvezan, A.J., Takahashi, H., Cantley, L.C., and Manning, B.D. (2014). Spatial control of the TSC complex integrates insulin and nutrient regulation of mTORC1 at the lysosome. Cell *156*, 771-785.

Middleton, K. and Carbon, J. (1994). KAR3-encoded kinesin is a minus-end-directed motor that functions with centromere binding proteins (CBF3) on an in vitro yeast kinetochore. Proc. Natl. Acad. Sci. U. S. A. *91*, 7212-7216.

Nguyen, T.P., Frank, A.R., and Jewell, J.L. (2017). Amino acid and small GTPase regulation of mTORC1. Cell. Logist. *7*, e1378794.

Nithianantham, S., Le, S., Seto, E., Jia, W., Leary, J., Corbett, K.D., Moore, J.K., and Al-Bassam, J. (2015). Tubulin cofactors and Arl2 are cage-like chaperones that regulate the soluble αβ-tubulin pool for microtubule dynamics. Elife *4*, e08811.

Noda, Y., Okada, Y., Saito, N., Setou, M., Xu, Y., Zhang, Z., and Hirokawa, N. (2001). KIFC3, a microtubule minus end-directed motor for the apical transport of annexin XIIIb-associated Triton-insoluble membranes. J. Cell Biol. *155*, 77-88.

Panchaud, N., Peli-Gulli, M.P., and De Virgilio, C. (2013). Amino acid deprivation inhibits TORC1 through a GTPase-activating protein complex for the Rag family GTPase Gtr1. Sci. Signal. *6*, ra42.

Paschal, B.M. and Vallee, R.B. (1987). Retrograde transport by the microtubule-associated protein MAP 1C. Nature *330*, 181-183.

Peng, M., Yin, N., and Li, M.O. (2017). SZT2 dictates GATOR control of mTORC1 signalling. Nature *543*, 433-437.

Porter, M.E., Scholey, J.M., Stemple, D.L., Vigers, G.P., Vale, R.D., Sheetz, M.P., and McIntosh, J.R. (1987). Characterization of the microtubule movement produced by sea urchin egg kinesin. J. Biol. Chem. *262*, 2794-2802.

Sancak, Y., Bar-Peled, L., Zoncu, R., Markhard, A.L., Nada, S., and Sabatini, D.M. (2010). Ragulator-Rag complex targets mTORC1 to the lysosomal surface and is necessary for its activation by amino acids. Cell *141*, 290-303.

Sarbassov, D.D., Guertin, D.A., Ali, S.M., and Sabatini, D.M. (2005). Phosphorylation and regulation of Akt/PKB by the rictor-mTOR complex. Science *307*, 1098-1101.

Saxton, R.A., Chantranupong, L., Knockenhauer, K.E., Schwartz, T.U., and Sabatini, D.M. (2016). Mechanism of arginine sensing by CASTOR1 upstream of mTORC1. Nature *536*, 229-233.

Scholey, J.E., Nithianantham, S., Scholey, J.M., and Al-Bassam, J. (2014). Structural basis for the assembly of the mitotic motor Kinesin-5 into bipolar tetramers. Elife *3*, e02217.

Sharp, D.J., McDonald, K.L., Brown, H.M., Matthies, H.J., Walczak, C., Vale, R.D., Mitchison, T.J., and Scholey, J.M. (1999). The bipolar kinesin, KLP61F, cross-links microtubules within interpolar microtubule bundles of Drosophila embryonic mitotic spindles. J. Cell Biol. *144*, 125-138.

Slangy, A., Lane, H.A., d'Hérin, P., Harper, M., Kress, M., and Niggt, E.A. (1995). Phosphorylation by p34cdc2 regulates spindle association of human Eg5, a kinesin-related motor essential for bipolar spindle formation in vivo. Cell *83*, 1159-1169.

Tseng, K.F., Wang, P., Lee, Y.J., Bowen, J., Gicking, A.M., Guo, L., Liu, B., and Qiu, W. (2018). The preprophase band-associated kinesin-14 OsKCH2 is a processive minus-end-directed microtubule motor. Nat. Commun. *9*, 1067.

Vale, R.D., Reese, T.S., and Sheetz, M.P. (1985). Identification of a novel force-generating protein, kinesin, involved in microtubule-based motility. Cell *42*, 39-50.

Wakana, Y., Villeneuve, J., van Galen, J., Cruz-Garcia, D., Tagaya, M., and

Malhotra, V. (2013). Kinesin-5/Eg5 is important for transport of CARTS from the trans-Golgi network to the cell surface. J. Cell Biol. *202*, 241-250.

Walker, R.A., Salmon, E.D., and Endow, S.A. (1990). The Drosophila claret segregation protein is a minus-end directed motor molecule. Nature *347*, 780-782.

Wang, X., Campbell, L.E., Miller, C.M., and Proud, C.G. (1998). Amino acid availability regulates p70 S6 kinase and multiple translation factors. Biochem. J. *334*(Pt 1), 261-267.

Wolfson, R.L., Chantranupong, L., Saxton, R.A., Shen, K., Scaria, S.M., Cantor, J.R., and Sabatini, D.M. (2016). Sestrin2 is a leucine sensor for the mTORC1 pathway. Science *351*, 43-48.

Wolfson, R.L., Chantranupong, L., Wyant, G.A., Gu, X., Orozco, J.M., Shen, K., Condon, K.J., Petri, S., Kedir, J., Scaria, S.M., et al. (2017). KICSTOR recruits GATOR1 to the lysosome and is necessary for nutrients to regulate mTORC1. Nature *543*, 438-442.

Yang, H., Jiang, X., Li, B., Yang, H.J., Miller, M., Yang, A., Dhar, A., and Pavletich, N.P. (2017). Mechanisms of mTORC1 activation by RHEB and inhibition by PRAS40. Nature *552*, 368-373.